IMC based Fractional Order Controller Design for Specific Non-Minimum Phase Systems

Pushkar Prakash Arya (*) **Sohom Chakrabarty** (**)

(*) *Indian Institute of Roorkee, Roorkee-247667, INDIA (e-mail: pushkarprakasharya@gmail.com)*
(**) *Indian Institute of Roorkee, Roorkee-247667, INDIA (e-mail: sohomfee@iitr.ac.in)*

Abstract: Internal model control (IMC) structure is derived from classical control by introducing the model of plant in the control loop and thereby having significant advantages over classical control such as dual stability, perfect control and zero-steady state offset. The basic one degree of freedom (ODF) IMC provides good compromise between set-point tracking and disturbance rejection and works well for non-minimum phase (NMP) systems. In this work, an IMC based fractional order (FO) controller is designed for NMP system which satisfy desired phase margin (ϕ_m) at a desired gain-crossover frequency (ω_g). The domain of desired ϕ_m and ω_g is provided from which they can be selected. Simulation studies are done for (i) DC-DC boost converter which is a NMP system with one zero in right half of s-plane and (ii) first order plus time delay (FOPTD) system which is also a NMP system because of the delay. Significance of the proposed methodology is verified by comparing with other well-known techniques in IMC based on the performance measures, such as rise time (T_r), settling time (T_s) and overshoot ($\%M_p$) and performance indices such as integral square error (ISE), integral absolute error (IAE) and integral of the time weighted absolute error ($ITAE$).

Keywords: Internal model control (IMC), fractional order (FO) control, non-minimum phase (NMP) systems, phase margin, gain cross-over frequency.

1. INTRODUCTION

Though the fractional order (FO) calculus is an old concept in mathematics, it is new in engineering domain. Only for last three decades application of FO is increasing in engineering as it is proved to be an effective way to represent physical systems and it provides more flexibility with more number of parameters to tune in controller design over their integer order (IO) counterpart (S. Das , 2011) . For example fractional order PID (FOPID) have five parameters to tune whereas integer order PID (IOPID) has only three, therefore the flexibility in design is more, and more specifications can be incorporated with the FOPID controller (Monje et al , 2010).

IMC is an old concept proposed by Garcia et al. (1982), Garcia et al. (1986) and Rivera et al. (1986), which incorporates the model of the plant in the control loop. IMC controller design technique is based on pole-zero cancellation, and the controller constitutes the inverse of the minimum phase part of the plant model and a filter. The order of the filter is such that the controller becomes proper (Morari & Zafiriou , 1989). This filter can be integer order (IO) or FO. In IO filter there is only one tuning parameter which is tuned to achieve satisfactory response of the systems, whereas FO filter provides one extra degree of freedom, i.e, the filter has two parameters to tune, therefore providing more flexibility in design. In this work FO filter is used and two parameters are tuned to satisfy desirable phase margin (ϕ_m) and gain-crossover frequency (ω_g) specifications simultaneously. With IO filter, however, only one of the above specifications can be satisfied (Morari & Zafiriou , 1989).

Since IMC is obtained by introducing the model of the plant in the control loop of the classical control structure, therefore IMC can be reduced to its equivalent classical control structure (Rivera et al. , 1986). However, IMC also has the advantage that it can provide simple and elegant solution to design H_2 optimal controller (Zhang et al. , 2006) in frequency domain, which is not possible using a classical controller. Though there are some advantages, however IMC also has its own issues to be taken care of. It is observed that with RHP zeros in the plant then model uncertainty amplifies high frequency noise as the overall system is sensitive with respect to change in plant at high frequencies. This noise amplification for systems with RHP zero can be avoided by designing IMC controller by first multiplying the numerator and denominator of the system transfer function by the conjugate of the RHP zero.

IMC has been proved to be successful in a wide area of control applications, such as process control (Datta et al. , 2015), (Li et al. , 2009), electrical drive systems (Sun et al. , 2016), (Zhu et al. , 2016), power systems (Tan , 2010), signal processing (Tan and Fu , 2016) and power electronics (Kobaku et al. , 2017), etc. Much research work has been carried out for analyzing and improving IMC such as anti-windup control design for IMC (Zheng et al. , 1993), for improving filter (Horn et al. , 1996), (Liu and Gao , 2010), H_∞ controller design for IMC (Dehghania et al. , 2006), adaptive IMC (Datta and Ochoa , 1996), (Datta and Xing , 1998), (Hu and Rangaiah , 1999), IMC for gain margin and phase margin specifications (Kaya , 2004), (Ho et al , 2001), etc.

IMC technique works very well for stable, minimum phase and NMP processes. But the design flexibility of the traditional IMC

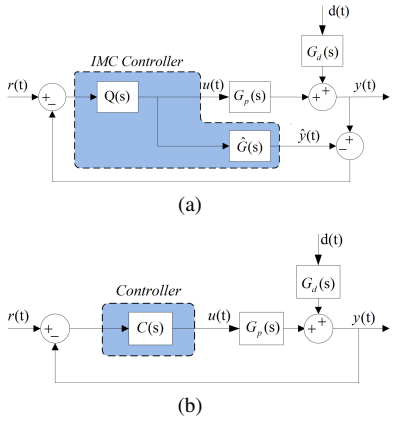

Fig. 1. (a) IMC control and (b) Equivalent classical control

with IO filter is limited because of the presence of only one tuning parameter. In this work a FO filter is proposed to increase the flexibility of the controller with two tuning parameters to satisfy independent choice in the selection of ϕ_m and ω_g. The significance of the proposed control strategy is verified on two different systems: (i) a DC-DC boost converter and (ii) a FOPTD system. The comparison are made for T_r, T_s, $\%M_p$ and performance are measured with performance indices, *ISE*, *IAE* and *ITAE*.

The contents of the paper are as follows: In Section-2, fundamentals of IMC is discussed. In Section-3, controller design steps and guidelines on selection of ϕ_m and ω_g and robustness is discussed and in Section-4 simulation studies with performance measures and discussion on the controller is done. In Section-5 conclusions are made.

2. FUNDAMENTALS OF IMC

The block diagram of IMC is given in Fig.1(a), which can be reduced to the classical control structure, as in Fig.1(b). $G_p(s)$ is the actual plant, $\hat{G}(s)$ is the plant model, $G_d(s)$ is a disturbance transfer function and $Q(s)$ is the IMC controller. The design of $Q(s)$ constitutes of two steps: (i) determination of the inverse of the minimum phase part of the process model and selection of the filter and (ii) finding the filter parameters for desired system performance.

The plant and plant model can be segregated into minimum phase and non-minimum phase parts as

$$G_p(s) = G_{pm}(s)G_{pa}(s) \tag{1}$$

$$\hat{G}(s) = \hat{G}_m(s)\hat{G}_a(s) \tag{2}$$

It is assumed that the plant model is known, therefore, $G_p = \hat{G}$ or $G_{pm} = \hat{G}_m$, and $G_{pa} = \hat{G}_a$. The subscript $'m'$ shows minimum-phase (MP) part and subscript $'a'$ shows NMP part of the plant. The controller $Q(s)$ is

$$Q(s) = f(s)(\hat{G}_m(s))^{-1} \tag{3}$$

where $(\hat{G}_m(s))^{-1}$ is inverse of the minimum phase part of the plant model and $f(s)$ is a filter. The order of the filter is such that it results in a proper $Q(s)$. In this work fractional filter is selected as

$$f(s) = \frac{1}{\lambda s^\beta + 1}, \quad \beta \in (0,2), \lambda > 0 \tag{4}$$

Since the filter design allows for tuning two parameters, ideally two design specifications form the above can be selected independently. In this work λ and β are tuned to satisfy desired phase margin and gain cross-over frequency of the controlled system. Note that when $\beta = 1$, we get the traditional IO filter, and only one design specification can be satisfied by tuning λ. So the classical IO filter is included as a subset of the FO filters.

The IMC controller can easily be converted into classical controller, as in Fig.1(b), where (Morari & Zafiriou , 1989)

$$C(s) = \frac{Q(s)}{1 - Q(s)\hat{G}(s)} \tag{5}$$

Substituting (3) in (5), the controller becomes

$$C(s) = \frac{f(s)}{1 - f(s)\hat{G}_a(s)}(\hat{G}_m(s))^{-1} \tag{6}$$

3. CONTROLLER DESIGN

Systems having one or more zeros in RHP are called NMP systems. Dead time or transport lag also has NMP character, as it has excessive phase lag in high frequencies. In this work two types of systems with NMP behavior are considered. First is a system with one RHP zero and the second is first order plus time delay (FOPTD). The controller is tuned to satisfy desired ϕ_m and ω_g. Mathematically the specifications can be written as,

Specification-I

$$arg[L(j\omega)]|_{\omega=\omega_g} = -\pi + \phi_m \tag{7}$$

Specification-II

$$|L(j\omega)||_{\omega=\omega_g} = 1 \tag{8}$$

where $L(s)$ is open loop transfer function referring to Fig.1(b), ϕ_m is desired phase margin and ω_g is desired gain cross-over frequency.

3.1 System-I

The first system is a second order system with one zero in RHP having transfer function model

$$G_p(s) = \frac{k(as+1)(-bs+1)}{s^2 + cs + d} \tag{9}$$

Assuming accurate modeling, i.e. $G_p(s) = \hat{G}(s)$, where $G_p(s)$ is the actual plant and $\hat{G}(s)$ is the model, the MP and NMP parts of the model can be segregated as

$$\hat{G}_m(s) = G_{pm}(s) = \frac{k(as+1)}{s^2 + cs + d} \tag{10}$$

and

$$\hat{G}_a(s) = G_{pa}(s) = -bs + 1 \tag{11}$$

The open loop transfer function (Fig.1(b)) is given as

$$L(s) = C(s)G_p(s) \tag{12}$$

Now, substituting $f(s)$ from (4) in (6) we have

$$C(s) = \frac{1}{\lambda s^\beta + 1 - \hat{G}_a(s)}\left(\hat{G}_m(s)\right)^{-1} \tag{13}$$

Therefore, open loop transfer function becomes

$$L(s) = \frac{G_a(s)}{\lambda s^\beta + 1 - \hat{G}_a(s)} \tag{14}$$

Substituting $\hat{G}_a(s) = G_{pa}(s) = -bs + 1$ from (11) in (14), we have

$$L(s) = \frac{-bs+1}{\lambda s^\beta + bs} \tag{15}$$

Substituting $s = j\omega$ in (15) we get

$$L(j\omega) = \frac{1 - j(b\omega)}{(\lambda\omega^{\beta}\cos(\frac{\beta\pi}{2})) + j(\lambda\omega^{\beta}\sin(\frac{\beta\pi}{2}) + b\omega)} \tag{16}$$

To satisfy ϕ_m and ω_g criteria, equation (16) should follow (7) and (8). From (7) and (16), we have

$$-\tan^{-1}(b\omega_g) - \tan^{-1}\left(\frac{\lambda\omega_g^{\beta}\sin\frac{\beta\pi}{2} + b\omega_g}{\lambda\omega_g^{\beta}\cos\frac{\beta\pi}{2}}\right) = -\pi + \phi_m$$

solving for λ in terms of β we get

$$\lambda = \frac{-b\omega_g}{\omega_g^{\beta}\left(\sin\frac{\beta\pi}{2} - A\cos\frac{\beta\pi}{2}\right)} \tag{17}$$

where $A = \tan(\pi - \phi_m - \tan^{-1}(b\omega_g))$. From (8) and (16) we have

$$\frac{\sqrt{1 + (b\omega_g)^2}}{\sqrt{\left(\lambda\omega_g^{\beta}\cos\frac{\beta\pi}{2}\right)^2 + \left(\lambda\omega_g^{\beta}\sin\frac{\beta\pi}{2} + b\omega_g\right)^2}} = 1$$

Simplifying above equation it will result into a quadratic equation in λ as

$$P\lambda^2 + Q\lambda + R = 0 \tag{18}$$

where, $P = \omega_g^{2\beta}$, $Q = 2b\omega_g^{\beta+1}\sin\frac{\beta\pi}{2}$ and $R = -1$ The roots of (18) is given as

$$\lambda = \frac{-Q \pm \sqrt{Q^2 - 4PR}}{2M} \tag{19}$$

Graphical technique is used to solve (17) and (19) simultaneously. A λ vs. β plot is obtained from (17) and (19) by varying $\beta \in (0,2)$. The intersection point of curve for (17) and the curve for (19) will be the solution, i.e, the set of obtained λ and β will satisfy (7) and (8) simultaneously. It can be noted that the range of β from 0 to 2 is observed to satisfy required conditions that (a) the IMC controller is proper, (b) the system is closed loop stable and (c) the solution exists for (17) and (18) to satisfy desired ϕ_m and ω_g.

Discussion-I: The controller $C(s)$ in (13) can be considered as PID controller plus a combination of IO and FO filter.
Proof: From (13) we have,

$$C(s) = \frac{1}{\lambda s^{\beta} + 1 - \hat{G}_a(s)}\left(\hat{G}_m(s)\right)^{-1} \tag{20}$$

substitute $e^{-\theta s} = -\theta s + 1$ and $\hat{G}_m(s)$ from (10), we get

$$C(s) = \frac{s^2 + cs + d}{\left(\lambda s^{\beta} + \theta s\right)k\left(as + 1\right)} \tag{21}$$

simplifying in form of PID and filter we can easily get

$$C(s) = K_{p1}\left(1 + K_{d1}s + \frac{1}{K_{i1}s}\right)\frac{1}{\left(T_{11}s^{\beta-1} + 1\right)\left(T_{12}s + 1\right)} \tag{22}$$

where, $K_{p1} = \frac{c}{\theta k}$, $K_{d1} = \frac{1}{c}$, $K_{i1} = \frac{c}{d}$, $T_{11} = \frac{\lambda}{\theta}$ and $T_{12} = a$.

3.2 System-II

A FOPTD plant can be written as

$$G_p(s) = \frac{k}{\tau s + 1}e^{-\theta s} \tag{23}$$

Assuming exact modeling of the plant, i.e. $\hat{G} = G_p$, where, $\hat{G}$ is the plant model and G_p is the actual plant, the minimum phase and non-minimum phase parts of the plant and plant model are

$$\hat{G}_m(s) = G_{pm}(s) = \frac{k}{\tau s + 1} \tag{24}$$

$$\hat{G}_a(s) = G_{pa}(s) = e^{-\theta s} \tag{25}$$

The open loop transfer function (Fig.1(b)) is given as

$$L(s) = C(s)G_p(s) \tag{26}$$

Substituting $f(s)$ from (4) in (6), we have

$$C(s) = \frac{1}{\lambda s^{\beta} + 1 - \hat{G}_a(s)}\left(\hat{G}_m(s)\right)^{-1} \tag{27}$$

Substituting $G_p(s)$ from (23) and $C(s)$ from (27) in (26), the open loop transfer function becomes

$$L(s) = \frac{G_{pa}(s)}{\lambda s^{\beta} + 1 - \hat{G}_a(s)} \tag{28}$$

Using first order Taylor series approximation of the delay term present in denominator (Kaya , 2004), $\hat{G}_a(s) = -\theta s + 1$ and substituting $G_{pa}(s) = e^{-\theta s}$ from (25) in (26), we get

$$L(s) = \frac{e^{-\theta s}}{\lambda s^{\beta} + \theta s} \tag{29}$$

Substituting $s = j\omega$ in (29), we get

$$L(j\omega) = \frac{e^{-j\theta\omega}}{\left(\lambda\omega^{\beta}\cos\frac{\beta\pi}{2}\right) + j\left(\lambda\omega^{\beta}\sin\frac{\beta\pi}{2} + \theta\omega\right)} \tag{30}$$

From (7) and (30) we have

$$-\theta\omega_g - \tan^{-1}\left(\frac{\lambda\omega_g^{\beta}\sin\frac{\beta\pi}{2} + \theta\omega_g}{\lambda\omega_g^{\beta}\cos\frac{\beta\pi}{2}}\right) = -\pi + \phi_m$$

Solving for λ, we have

$$\lambda = \frac{-\theta\omega_g}{\omega_g^{\beta}\left(\sin\frac{\beta\pi}{2} - A\cos\frac{\beta\pi}{2}\right)} \tag{31}$$

where $A = \tan(\pi - \phi_m - \theta\omega_g)$. Now, from (8) and (30)

$$\frac{1}{\sqrt{\left(\lambda\omega_g^{\beta}\cos\frac{\beta\pi}{2}\right)^2 + \left(\lambda\omega_g^{\beta}\sin\frac{\beta\pi}{2} + \theta\omega_g\right)^2}} = 1$$

Simplifying above equation in terms of λ will result in a quadratic equation as

$$P\lambda^2 + Q\lambda + R = 0 \tag{32}$$

where $P = \omega_g^{2\beta}$,$Q = 2\theta\omega_g^{\beta+1}\sin\frac{\beta\pi}{2}$ and $R = (\theta\omega_g)^2 - 1$. The roots of (32) will give λ in terms of β as

$$\lambda = \frac{-Q \pm \sqrt{Q^2 - 4PR}}{2P} \tag{33}$$

Using graphical technique, λ and β can be obtained from (31) and (33) in the similar manner as obtained in $System - I$.

Discussion-II: The controller for System-II (in (27)) can be assumed as a combination of PI controller and a FO filter.
Proof: We have $C(S)$ from (27) as

$$C(s) = \frac{1}{\lambda s^{\beta} + 1 - \hat{G}_a(s)}\left(\hat{G}_m(s)\right)^{-1} \tag{34}$$

Substituting $e^{-\theta s} = -\theta s + 1$ and $\hat{G}_m(s)$ from (24) we get

$$C(s) = \frac{\tau s + 1}{k\left(\lambda s^{\beta} + \theta s\right)} \tag{35}$$

Simplify (35) in terms of PI and a FO filter we get

$$C(s) = K_{p2}\left(1 + \frac{1}{K_{i2}s}\right)\frac{1}{\left(T_2 s^{\beta-1} + 1\right)} \tag{36}$$

where, $K_{p2} = \frac{\tau}{\theta k}$, $K_{i2} = \tau$ and $T_2 = \frac{\lambda}{\theta}$.

3.3 Guidelines for selection of ϕ_m and ω_g

The concepts of sensitivity and complementary sensitivity forms the basics of robustness and stability of systems. Complementary sensitivity transfer function reflects tracking action and sensitivity transfer function reflects disturbance rejection capability and robustness of the system. From Fig.1(b), the response of the system is given by, $Y(s) = T(s)R(s) + S(s)G_d(s)D(s)$, where $S(s)$ is sensitivity transfer function and $T(s)$ is complementary sensitivity transfer function given as:

$$S(s) = \frac{1}{1 + G_p(j\omega)C(j\omega)} \tag{37}$$

and

$$T(s) = \frac{G_p(j\omega)C(j\omega)}{1 + G_p(j\omega)C(j\omega)} \tag{38}$$

Maximum sensitivity is a measure of robustness given as $M_s = \max_{\omega} S(s)$. Generally $M_s \in (1,2)$ (Astrom and Hagglund , 2006) gives good combination of disturbance rejection, set-point tracking and robustness of the system. Higher M_s results in faster performance but poor robustness, whereas small M_s gives sluggish response and highly robust system. The relation between M_s and phase margin (PM) and gain margin (GM) is (Skogestad & Ian , 2001)

$$PM \geq 2\sin^{-1}\left(\frac{1}{2M_s}\right)$$

and

$$GM \geq \frac{M_s}{M_s - 1}$$

For $M_s \in (1,2)$ we get $PM \in (60, 28.955)\,deg$ and $GM \in (\infty, 2)$. To have good satisfactory set-point tracking and robustness, $PM \in (30,60)$ can be chosen (Skogestad & Ian , 2001).

Gain cross-over frequency (ω_g) determines the speed of response. But higher ω_g demands higher control input. Higher ω_g results in high bandwidth unless the cut-off rate of the closed loop system is very low, which happens when β is very small, say 0.1, but this cannot happen as small β would not provide enough phase to the system to satisfy desired ϕ_m. So higher ω_g results in larger bandwidth which results in higher control input. This may cause the control to exceed the maximum limit of the actuator. However, if T_1 is the time for which the control signal is high, and T_c is the time constant of the system then it is observed that for $T_1 << T_c$, the higher control input can be limited by using a saturation block without affecting system dynamics (the effect of saturation is almost negligible). Also for higher ω_g, there might not be any $\lambda > 0$ and $\beta \in (0,2)$ which satisfy desired $\phi_m \in (30,60)$.

Based on the above ideas, the desired phase margin and gain cross-over frequency are selected.

4. SIMULATION STUDIES

4.1 System-I

A boost converter transfer function model is taken form Kobaku et al. (2017) where a two-degree-of-freedom (TDF) IO-IMC is designed. The system transfer function is given as

$$G_p(s) = \frac{1.65318 \times 10^8 (1.5544 \times 10^{-4} s + 1)}{(-7.8087 \times 10^{-5} s + 1)} \\ \overline{s^2 + 141.2289 s + 7.4934 \times 10^4}$$

Table 1. Performance measures for System-I.

	$T_r\,(sec)$	$T_s\,(sec)$	$\%M_p$	ISE	IAE	$ITAE$
Proposed	0.0019	0.0096	15.6354	0.001415	0.00563	0.01648
Kobaku et al	0.0185	0.0322	0.0000	0.008404	0.01648	0.00097

Source voltage and load current variations are two major source of disturbances in DC-DC boost converter. Since change in source voltage dominantly affects the output voltage than the output current, only disturbance due to source voltage is considered in this context to make the paper concise and at the same time justifying the significance of the proposed control strategy. The disturbance transfer function of output voltage to source voltage is given as, (Kobaku et al. , 2017),

$$G_d(s) = \frac{1.486(1.544 \times 10^{-4} s + 1)}{1.3345 \times 10^{-5} s^2 + 1.8847 \times 10^{-3} s + 1}$$

With two unknowns in FO controller (λ and β), the controller is tuned for $\phi_m = 60\,deg$ and $\omega_g = 650\,rad/sec$. Following controller design steps given in *Section-3.1*, the value of unknown parameters obtained are $\beta = 1.3164$ and $\lambda = 1.8965 * 10^{-4}$ (Fig.2(a)). Therefore, the equivalent classical controller transfer function is given as

$$C(s) = \frac{s^2 + 141.2289 s + 7.4934 \times 10^4}{(257 s + 1.653 \times 10^6)} \\ \overline{(1.8965 \times 10^{-4} s^{1.3164} + 7.8287 \times 10^{-5} s)}$$

For the simulation, 8^{th} order Oustaloup approximation in the range of $\omega \in (10, 10000)$ (Monje et al , 2010) is used to implement the FO controller. The Bode plot of system-I is shown in Fig.2(a). The phase margin and gain cross-over frequency of the controlled system is very near to the desired and the mismatch can be attributed to the approximation used for realizing the FO term in the controller (i.e. s^{β}). The controller is tuned for higher $\omega_g = 650\,rad/sec$ to have faster response than in Kobaku et al. (2017) which uses $\omega_g = 600\,rad/sec$. Therefore speed of response with the proposed controller is faster. Note that $M_s = 1.4$ for the proposed controller whereas in Kobaku et al. (2017) $M_s = 1.235$. Both are within a tolerable bound.

As no disturbance rejection controller is used in the proposed scheme, the disturbance rejection is poor with oscillations appearing in the response. With disturbance rejection controller in Kobaku et al. (2017), the controller avoids overshoot while rejecting disturbance from the control loop, But the undershoot for disturbance is more. For comparison, transient response rise time (T_r), settling time (T_s) and overshoot $(\%M_p)$ are compared in Table-1, and also ISE, IAE and $ITAE$ performance measures are compared. It is observed that the proposed IMC based FO controller performs better than two degree of freedom IO-IMC in terms of T_r, T_s, ISE and IAE. The performance indices are found with disturbance $(= -0.7$ at $0.15\,sec)$ and total time of simulation is $0.3\,sec$. Simulations are also performed to compare the ODF-FO IMC with ODF-IO IMC and it was seen that the ODF-FO IMC controller performed better for all performance measures. These plots are not shown to make the paper concise.

4.2 System-II

A FOPTD system model is considered from Kaya (2004). The plant transfer function is given as

$$G_p(s) = \frac{e^{-1.34s}}{1.44s + 1}$$

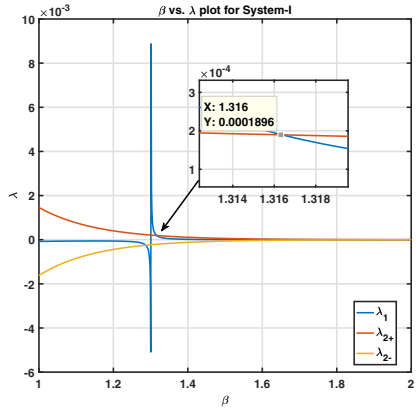

(a)

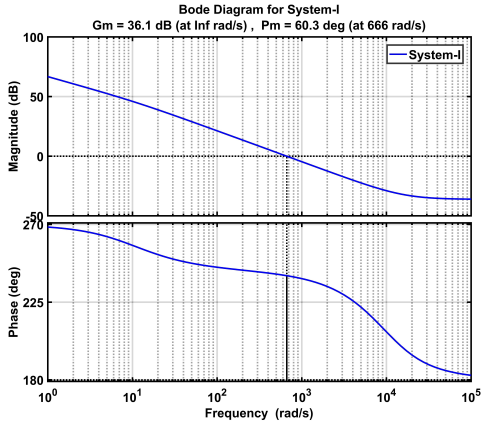

(b)

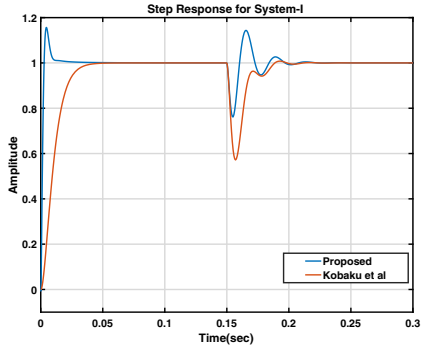

(c)

Fig. 2. System-I: (a) β vs. λ plot using (17), (λ_1) and (19), (λ_{2+} and λ_{2-}) (b) Bode diagram of the system with proposed controller and (c) Step response of the system with different controllers.

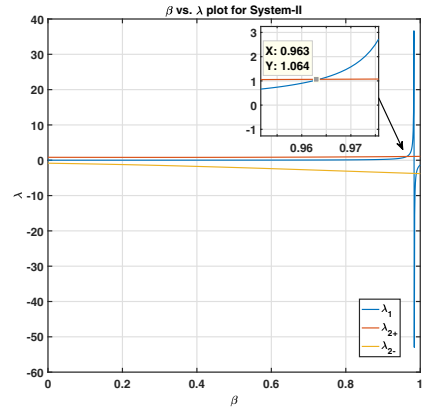

(a)

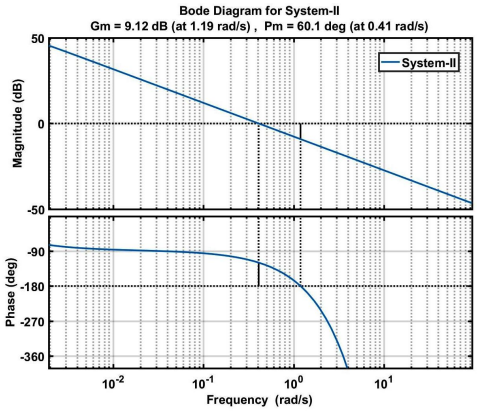

(b)

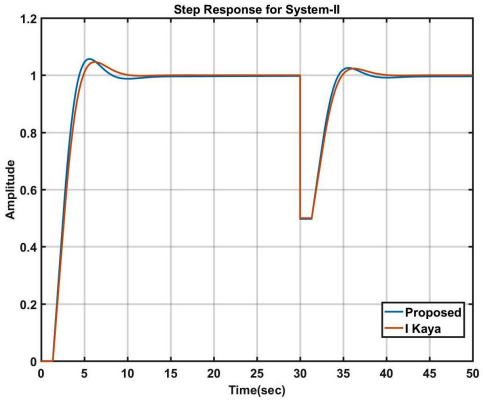

(c)

Fig. 3. System-II: (a) β vs. λ plot, using (31), (λ_1) and (33), (λ_{2+} and λ_{2-}) (b) Bode diagram of the system with proposed controller and (c) Step response of the system with different controllers.

In Kaya (2004), the controller design provides phase margin of $60.9\,deg$ and gain cross-over frequency of 0.379. In this work, the controller is designed for $\phi_m = 60\,deg$ and $\omega_g = 0.41\,rad/sec$. Following $Section - 3.2$, we get $\lambda = 1.0648$ and $\beta = 0.9636$ (Fig.3(a)). Therefore, the controller transfer function becomes

$$C(s) = \frac{1.44s + 1}{1.0648s^{0.9636} + 1.34s}$$

Eighth order Oustaloup approximation in $\omega \in (0.001, 1000)$ is used to implement fractional order term in the controller. Bode plot and step response is given in Fig.3. Performance measures are tabulated in Table-2. The proposed method outperforms Kaya (2004) in terms of T_r, T_s, ISE, IAE and $ITAE$. The maximum sensitivity for proposed control loop is 1.6943 which is comparable to Kaya (2004), where it is 1.6051. Since no disturbance rejection controller is used, the disturbance rejection profile is similar in both the cases and only the set-point controller ($C(s)$) handles the disturbance.

Table 2. Performance measures for System-II.

	$T_r\,(sec)$	$T_s\,(sec)$	$\%M_p$	*ISE*	*IAE*	*ITAE*
Proposed	2.2082	7.3604	5.888	2.158	2.936	10.64
I Kaya	2.4850	8.1577	4.628	2.807	4.343	51.24

5. CONCLUSIONS

This paper proposes a IMC based FO controller to design for independently specified phase margin and gain-crossover frequency. A FO filter is used in place of IO filter, thereby introducing an extra parameter which is used to tune the desired specifications.

A graphical technique is proposed to obtain the parameter values for the given specification on phase margin and gain cross-over frequency. Furthermore, the operational ranges for these specifications are also given from maximum sensitivity viewpoint.

The proposed technique is verified for two different kind of systems, taken from well cited references (Kobaku et al. (2017) and Kaya (2004)). First system is a DC-DC boost converter which is NMP system with one zero in RHP and second is a FOPTD process model. The superiority of adding extra degree-of-freedom in controller is verified through simulations for set-point changes and disturbance rejection. The proposed controller gives better results in almost all performance indices.

In ODF-IO IMC, only one tuning parameter cannot satisfy more than one specification at a time. Even if they do then the desired specifications are related with a relation, as in Kaya (2004). On the other hand, with the proposed methodology for designing ODF-FO IMC, the response can be improved by independently selecting desired ϕ_m and ω_g. This can be seen both in system-I and system-II.

REFERENCES

Astrom K. J. & Hagglund T., (2006), *Advanced PID control*, ISA-The Instrumentation, Systems, and Automation Society. Research Triangle Park, NC 27709.

Das S., (2011), *Functional Fractional Calculus*, Berlin, Springer.

Datta A. & Ochoa J., (1996) "Adaptive Internal Model Control: Design and Stability Analysis", *Automatica*, 32(2), 261-266.

Datta A. & Xing L., (1998), "The Theory and Design of Adaptive Internal Model Control Schemes", *Proc. of the American Cont. Conf.*, Philadelphia, Pennsylvania.

Datta S., Nath U.M. & Dey C., (2015), "Design and implementation of decentralized IMC-PI controllers for real time coupled tank process", *MFIIS*.

Dehghania A., Lanzona A. & B. D.O. Anderson, (2006), " H_∞ design to generalize internal model control", *Automatica*, 42, 1959-1968.

Garcia C. E. & Morari M. , (1982), "Internal model control. 1. A unifying review and some new results", *Industrial & Engineering Chemistry Process Design and Development*, 21(2), 308-323.

Garcia C. E. & Morari M., (1986), "Internal model control. 2. Design procedure for multivariable systems", *Ind. Eng. Chem. Process Design Development*, 24(2), 472-84.

Horn I. G., Arulandu J. R., Gombas C. J., Antwerp J. G. V. & Braatz R. D., (1996), "Improved Filter Design in Internal Model Control",*Ind. Eng. Chem. Res.*, 35, 3437-3441.

Ho W. K., Hang C. C. & Cao L., (1995), "Tuning of PID controllers based on gain and phase margin specifications", *Automatica*, 31, 497-502.

Ho W. K., Lee T. H., Han H. P., & Hong Y., (2001), "Self-Tuning IMC-PID Control with Interval Gain and Phase Margins Assignment", *IEEE Trans. on Cont. Sys. Techn.*, 9(3).

Hu Q. & Rangaiah G. P., (1999), "Adaptive internal model control of nonlinear processes", *Chem. Engg. Science*, 54, 1205-1220.

Kaya I., (2004), "Tuning PI controllers for stable processes with specifications on gain and phase margins", *ISA Transactions*, 43, 297-304.

Kobaku T., Patwardhan S. C. & V. Agarwal, (2017), "Experimental Evaluation of Internal Model Control Scheme on a DC-DC Boost Converter Exhibiting Nonminimum Phase Behavior", *IEEE Trans. on Power Electronics*, 32(11).

Li D., Zeng F., Jin Q., & Pan L., (2009), "Applications of an IMC based PID Controller tuning strategy in atmospheric and vacuum distillation units", *Nonlinear Analysis: Real World Applications*, 10, 2729-2739.

Liu T. & Gao F., "New insight into internal model filter design for load disturbance rejection", *IET Control Th. Appl.*, 4(3), 448-460.

Morari M. & Zafiriou E., (1989) *Robust Process Control*, Prentice-Hall, Englewood Cliffs, NJ.

Monje C. A., Chen Y. Q., Blas M. & Feliu V., (2010), Fractional-order Systems and Controls: Fundamentals and Applications, *Springer*.

Rivera D. E. , Morari M. & Skogestad S., (1986), "Internal model control. 4. PID controller design", *Ind. Eng. Chem. Process Design Development*, 25(1), 252-65.

Skogestad S. & Ian P., (2001), *Multivariable Feedback Control Analysis and Design*, Hohn Wiley & Sons.

Sun X., Shi Z., Chen L., & Yang Z., (2016), "Internal Model Control for a Bearingless Permanent Magnet Synchronous Motor Based on Inverse System Method", *IEEE Trans. on Energy Conversion*, 31(4).

Tan W., (2010), "Unified Tuning of PID Load Frequency Controller for Power Systems via IMC", *IEEE Trans. on Power Systems*, Vol. 25(1).

Tan W. & Fu C., (2016), "Linear Active Disturbance-Rejection Control: Analysis and Tuning via IMC", *IEEE Trans. on Inds. Electronics*, 63(4).

Zheng A. , Kothare M. V. & Morari M., (1993), "Anti-Windup Design for Internal Model Control", *Tech. Memorandum on CIT-CDS*, 007.

Zhang W., Ou L. and Gu D., (2006), "Algebraic Solution to H_2 Control Problems. I. The Scalar Case", *Ind. Eng. Chem. res.*, 45, 7151-7162.

Zhou K., Doyle K. C. and Glover K., (1996), *Robust and Optimal Control*, Prentice Hall: Englewood Cliffs, NJ.

Zhu Q. , Yin Z., Zhang Y., Niu J., Li Y., & Zhong Y., (2016), "Research on Two-Degree-of-Freedom Internal Model Control Strategy for Induction Motor Based on Immune Algorithm", *IEEE Trans. on Inds. Electronics*, 63(3).